Imaging high-energy astrophysical sources using Earth occultation

S. N. Zhang*†, G. J. Fishman*, B. A. Harmon* & W. S. Paciesas*‡

* NASA Marshall Space Flight Center, Code ES66, Huntsville, Alabama 35812, USA
† Universities Space Research Association, Huntsville, Alabama 35806, USA
‡ University of Alabama in Huntsville, Huntsville, Alabama 35899, USA

HIGH-ENERGY astrophysical sources can be difficult to image. Photons with energies above ~5 keV are hard to focus, so experiments usually employ coded masks[1–4] or moving collimators[5–9] to modulate the flux received by the detectors; the resulting signals are then deconvolved to form the images. Here we demonstrate a new approach which makes use of the large-area, non-collimated detectors of the Burst and Transient Source Experiment on the Compton Gamma-Ray Observatory. As the spacecraft moves in its orbit, the Earth itself acts as a stable occulting disk. Changes in the measured signal during a single occultation correspond to the integrated intensity of sources positioned along the arc described by the Earth's edge (limb). The low-altitude, moderately inclined orbit of the spacecraft ensures that the angle at which the limb traverses a source region varies between occultations, and thus data from a series of occultations can be transformed into an image. This imaging process is conceptually and mathematically similar to those used in fan-beam aperture-synthesis radio-astronomy[10] and medical computer-assisted tomography[11], and holds great promise for all-sky imaging with relatively simple (and hence inexpensive) detectors.

In visible-wavelength optics, transform imaging has been described for at least the past 30 years[12,13], although it has not seen widespread applications. For high-energy astronomy, transform-imaging processes are reviewed by Caroli *et al.*[7] and by Lei *et al.*[14] The coded-aperture imager produces a spatially modulated signal, whereas the rotation-modulation imager produces a temporal modulation. The modulated signal from the detector is later deconvolved to produce an image. A variant of the rotation-modulation imager is a scanning-modulation imager, in which scans of the imaged region are made along different scan angles. Experiments on previous spacecraft such as Uhuru, SAS-3, Ariel-5 and HEAO-1 have used 'lines of position' perpendicular to the scan directions of a collimator to locate point sources. They could not, however, obtain a true transformed image of a region (as is obtained here) because of the limited number of scan directions available and/or the long time between scans. These previous techniques also require a pointed or scanning mask with a size comparable to that of the detector. The field-of-view is limited by the mask size, and the angular resolution is limited by the distance between the mask and detector.

Our technique uses the Earth's limb as a well defined, stable occulting disk. We call this process occultation-transform imaging. The features of the three imaging techniques are compared in Table 1. This technique is demonstrated using the large-area detectors of the Burst and Transient Source Experiment[15] (BATSE) on the Compton Gamma-Ray Observatory (GRO). The typical resolution (point-spread function) for the BATSE occultation-imaging system is ~0.5° and the positional accuracy is ~0.1°. A significant component of the positional error results from the limited time resolution of the BATSE data. Another component, of comparable magnitude, results from the 'fuzziness' of the Earth's limb (arising from the atmosphere) as sources are occulted. In principle, this latter source of image degradation can be reduced as the grazing atmospheric transmission can be accurately modelled as a function of energy.

At a typical GRO altitude of 400 km, the Earth's limb for occultation is about 2,000 km away and lies about 70 km above the Earth's surface for γ-rays of energy 100 keV and approximately 65 km above the Earth at 1 MeV. The limb is about 108° from the zenith. At any given instant, the Earth subtends 34% of the total solid angle, as seen from the spacecraft. Throughout one orbit, sources in approximately 70% of the sky can produce two useful occultations per orbit (emergence/immersion or rise/set). As the GRO orbit precesses (with a period of 53 days), both of these occultation angles change in a continuous manner. For a low-altitude spacecraft with a moderate inclination, all sky regions eventually undergo occultation as the orbit precesses. The GRO orbit is inclined 28.5° with respect to the Earth; occultations are obtained for sources >47° from the orbital poles, but the available scanning time for sources near the celestial poles is reduced by about 30% relative to that of other sky regions.

Observations of sources by occultation were planned by the BATSE group before launch[15]. The original BATSE occultation method was one-dimensional in nature, or combined two or more one-dimensional scans across the source region to isolate and locate the source under study. It can be used only for well separated, relatively strong sources.

Our imaging process is an extension of the one-dimensional technique. When the limb of the Earth (an arc) sweeps through

TABLE 1 Comparison of hard X-ray/γ-ray imaging techniques for astronomy

	Coded-aperture transform imaging	Rotation- (or scanning-) modulation imaging	Occultation-transform imaging
Experiment–spacecraft	SIGMA–GRANAT	WATCH–GRANAT	BATSE–GRO
Field-of-view	$\sim 10^\circ \times 10^\circ$	$\sim 120^\circ$ FWHM (per detector)	Whole-sky (8 detectors)
Mask	50% opaque 2-D array	50% opaque slat mask	No mask (Earth limb)
Modulation produced by:	Stationary mask	Rotating (or scanning) mask, grid or slats	Spacecraft orbital motion; orbit precession
Sensitivity at edge of field	Low	Low	High
Position sensitive detector:	Required	Not required	Not required
Energy limitations:	Mask transmission, detector response	Mask transmission, detector response	Detector response
Inherent limitations on angular resolution	Detector spatial resolution, mask element size, mask-detector separation	Slat size, slat-detector separation	Earth limb location and model
Inherent limitations on temporal resolution	No limitation	Mask rotation (scan) period	Orbital period
References (Typ.)	1–4, 7, 14	5–9, 14	This paper

a chosen region of the sky, the detectors record the counting rate as a function of time. The occultation of a source is typically detected as a small ($\lesssim 1\%$) but rapid change in the counting rate in a detector. This occurs over a time of about $8/\cos\beta$ seconds, where β is the angle of the source with respect to the orbital plane. The location of the spacecraft is well known and thus the location and orientation of the limb projected on the sky can be determined accurately. The counting rate produced as the limb traverses a source region is differentiated. This becomes a signal indicative of the intensity of the sources integrated along the arc. This signal, representing a continuous series of arcs at different projection angles, is used as the input to the Radon transformation[11,16,17], which inverts the data to produce an image. This resembles computer-assisted tomographic imaging in that both processes require a large set of input source angles to reconstruct a reasonable image. For the present work, we have used the maximum-entropy software package of the Donner algorithm for Radon transform imaging[16]. Numerous images have been produced with fields ranging from 5° to 40° on a side. For larger regions, the Radon transformation is not well behaved and the images are highly distorted.

The technique is demonstrated in a series of images in two sky regions. The first region is a wide ($40^\circ \times 40^\circ$) field which includes a strong, stable source (the Crab Nebula) and the intense, transient hard X-ray source GRO J0422 + 32 discovered by the BATSE experiment in August 1992[18,19]. Three images are shown (Fig. 1*a–c*) of the same region, at different times. Figure 1*a* was made during the rising part of the outburst (intensity ~0.05 Crab); Fig. 1*b* was near the peak of the outburst (~3 Crab); and Fig. 1*c* (~1 Crab) was made during the declining phase. The offset of the image contours from the true source locations (shown by crosses) results from the distortion of the very wide field of the image. This offset is removed as the field is reduced. Images of strong sources have been positioned to within 0.1° in narrower-field (5°) images. Elongation of the contours around the point sources is a result of incomplete transformation, which stretches the contours along the direction of the Earth's limb.

The second region is a $20^\circ \times 20^\circ$ field near the Galactic Centre (Fig. 2). Four images are shown in this figure, taken at different times. The extreme variability of the hard X-ray sources in this region is evident and has been noted by other experiments with imaging capabilities[20–28]. From these images, only two sources in Fig. 2*c* and 2*d*, namely GX354−00 and 1E1740.7−2942, were unambiguously isolated and identified. GX1+4, shown in Fig. 1*a*, was also shown to be detected from other images produced with slightly different fields in the same period. This is in good

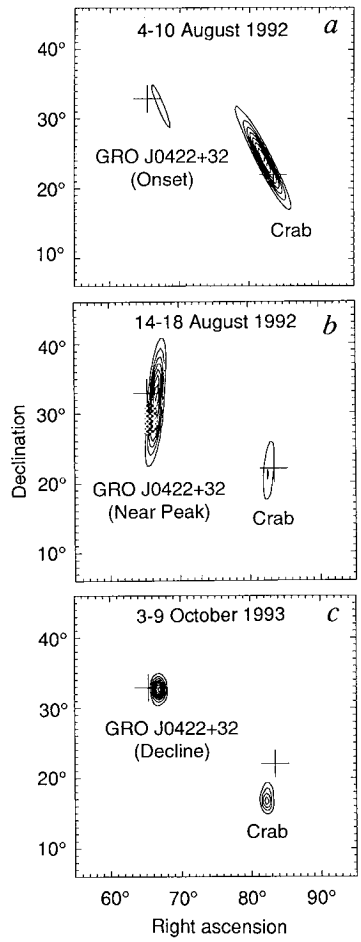

FIG. 1 *a–c*, The sky region containing the Crab Nebula and the intense, transient source GRO J0422+32 (Nova Persei 1992) at three different times during its outburst. These images have been produced by the method described in the text. A nonlinear, maximum-entropy processing of the images results in image contours that are not related to the absolute flux values, but instead indicate the relative intensity of sources within the field. The wide field of these images causes distortion such that the image contours are offset from the actual source locations (crosses). Narrow-field images of regions of strong sources yield contours that are within 0.1° of the actual location. The energy range for these images is 50 to 100 keV. The image size is $40^\circ \times 40^\circ$.

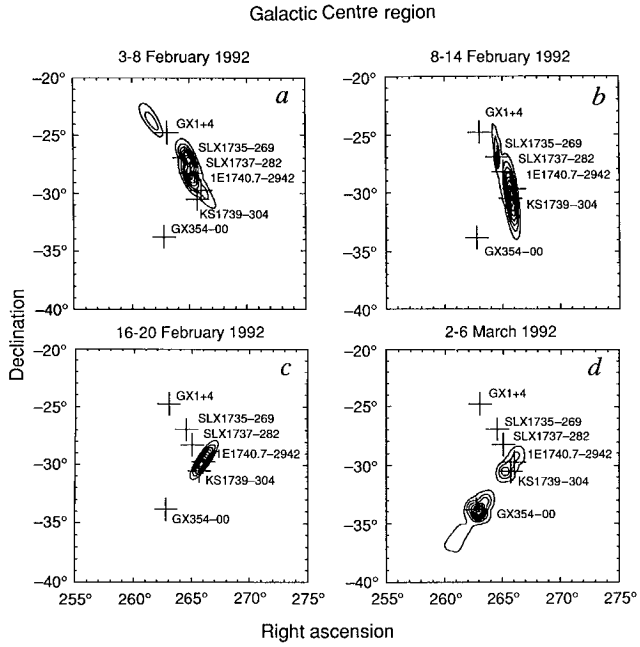

FIG. 2 *a–d*, Images of the Galactic Centre region (20° × 20°) at four different times, showing at least four variable sources. The intense state of GX354-00 in Fig. 2*d* is consistent with observations of the SIGMA experiment on the GRANAT spacecraft. The variability of other sources has not been observed independently during these times. The crosses show the actual location of sources observed previously. As in Fig. 1, the source locations are offset because of the wide field of these images and because there are other sources present in the field. Elongation of image contours in Figs 1 and 2 arises from incomplete or unfavourable occultation angles during the observations.

agreement with SIGMA/GRANAT observations in the similar periods[28]. The complex around the centre of the field shown in Fig. 2*a* and 2*b* agrees qualitatively with the significant detections of SLX1735−269 and 1E1740.7−2942 and the marginal detections of SLX1737−282 and KS1739−304 by SIGMA/GRANAT[28]. The present imaging system does not allow them to be separated unambiguously.

There are several instrumental considerations that make this technique particularly attractive for space-borne applications. There is no need for a large, massive mask and its support structure. Similarly, there are only minimal pointing requirements: the occulting disk (the Earth's limb) is stable, and it is sufficiently dense that it can be used effectively for higher-energy γ-rays. The greatest advantage of this technique over a coded-mask imager is that a position-sensitive detector is not required. An advantage over a rotation-modulation collimator is that there are no moving parts in the system, which have caused reliability problems in previous space-borne experiments. Other transform techniques have greatly reduced sensitivity when the source region is near the edge of the field. With occultation-transform imaging, there is no mask to restrict the field-of-view or reduce the off-axis sensitivity. The octahedral geometry of the BATSE detectors assures that high sensitivity can be achieved for source regions over the entire sky. Finally, for any imaging system utilizing a mask, the orientation of the mask with respect to the celestial sphere must be determined at all times. With the present technique, only the location of the spacecraft with respect to the Earth's limb need be determined to the required accuracy.

Many transient and highly variable sources, both galactic and extragalactic, vary on timescales observable by this imaging system—several days to years. Narrower-field instruments, of necessity, have a low observational duty cycle and thus have limited monitoring capability for most regions of the sky. The typical sensitivity achieved thus far is about 50 mCrab for a 1-week observation, as determined by observations of GRO J0422+32 during its declining phase.

Data analysis efforts are underway to process the large data set obtained by BATSE since launch (April 1991) and to image regions over the entire sky. Detection sensitivity, image quality and resolution are expected to improve beyond the preliminary images shown here as the background systematics become better known and as more-advanced image processing techniques are used with the data. As the BATSE detectors were designed for the study of γ-ray bursts, they are not optimized for this imaging application. Future high-energy astronomy experiments utilizing this technique can be improved greatly by using low background detectors and by collimating the detectors to view only a field around the horizon. This in turn, could permit the use of a simple, passive, gravity-gradient-stabilized spacecraft. □

Received 2 April; accepted 9 September 1993.

1. Fenimore, E. E. & Cannon, T. M. *Appl. Opt.* **17,** 337–347 (1978).
2. Skinner, G. K. *Nucl. Instrum. Meth.* **221,** 33–40 (1984).
3. Kohman, T. P. *Rev. Scient. Instrum.* **60**(11), 3396–3409 (1989).
4. Skinner, G. K. *Scient. Am.* **259**(2), 84–89 (August 1988).
5. Durouchoux, P., Hudson, H., Hurford, G., Hurley, K., Matteson, J. & Orsal, E. *Astr. & Astrophys.* **120,** 150–155 (1983).
6. Mertz, L. N., Nakano, G. H. & Kilner, J. R. *J. Opt. Soc. Am. A,* **3,** 2167–2170 (1986).
7. Caroli, E., Stephen, J. B., DiCocco, G., Natalucci, L. & Spizzichini, G. *Space Sci. Rev.* **45,** 349–403 (1987).
8. Willmore, A. P. *Mon. Not. R. Astr. Soc.* **147,** 387–403 (1970).
9. Cruise, A. M. *Mon. Not. R. Astr. Soc.* **170,** 305–312 (1975).
10. Bracewell, R. N. *Aust. J. Phys.* **9,** 198–217 (1956).
11. Gullberg, G. T. & Tsui, B. M. W. *Information Processing in Medical Imaging* (eds deGraaf, C. N. & Viergeren, M. A.) 181–189 (Plenum Press, New York, 1989).
12. Mertz, L. *Transformations in Optics* (Wiley, New York, 1965).
13. Mertz, L. in *Proc. EUV, X-ray and Gamma Ray Instrumentation for Astronomy and Atomic Physics, SPIE* **1159,** 14–17 (1989).
14. Lei, F., Fraser-Mitchell, J. & Yearworth, M. *Expl. Astr.* **1,** 285–303 (1991).
15. Fishman, G. J. *et al.* in *Proc. Gamma-Ray Observatory Science Workshop* (ed. Johnson, W. N.) 39–50 (NASA/GSFC, Greenbelt, MD, 1989).
16. Huesman, R. H. *et al. Donner Algorithms for Reconstruction Tomography. LBL Publ.* **214,** 42–44 (University of California, Berkely, 1977).
17. Deans, S. R. *The Radon Transform and Some of Its Applications* (Wiley, New York, 1983).
18. Harmon, B. A. *et al. IAU Circ. No.* 5781 (1993).
19. Harmon, B. A. *et al.* in AIP Conf. Proc. **280,** 314–318 *Compton Gamma Ray Observatory* (eds Friedlander, M., Gehrels, N. & Macomb, D.) (1993).
20. Skinner, G. K. *et al. Nature* **330,** 544–547 (1987).
21. Claret, A., Goldwurm, A., Cordier, A. & Paul, J. *Astrophys. J.* (in the press).
22. Cook, W. R. *et al. Astrophys. J.* **372,** L75–L81 (1991).
23. Sunyaev, R. *et al. Astr. Astrophys.* **247,** L29–L32 (1991).
24. Sinner, G. *Astr. Astrophys. Suppl. Ser.* **97,** 149–153 (1993).
25. Grindlay, J. E., Covault, C. E. & Manandhar, R. P. *Astr. Astrophys. Suppl. Ser.* **97,** 155–158 (1993).
26. Bazzano, L. *et al. Astr. Astrophys. Suppl. Ser.* **97,** 169–171 (1993).
27. Cordier, B. *et al. Astr. Astrophys. Suppl. Ser.* **97,** 177–180 (1993).
28. Churazov, E. *et al. Astr. Astrophys. Suppl. Ser.* **97,** 173–176 (1993).
29. Paciesas, W. S. *et al.* in AIP Conf. Proc. **280,** 473–477 *Compton Gamma Ray Observatory* (eds Friedlander, M., Gehrels, N. & Macomb, D.) (1993).

ACKNOWLEDGEMENTS. We are grateful for the help of the BATSE operations and data analysis teams. We have benefited from discussions with M. Finger, B. Rubin, C. Meegan and R. Wilson. We thank R. H. Huesman for providing the Donner algorithms.